138 | Y. Sun, J. K. Paik, A. Koschan, and M. A. Abidi, "3D reconstruction of indoor and outdoor scenes using a mobile range scanner," Proc. Int. Conf. Pattern Recognition, Canada, Vol. III, pp. 653-656, Quebec, Canada, August 2002.

3D Reconstruction of Indoor and Outdoor Scenes Using a Mobile Range Scanner

Y. Sun, J. K. Paik, A. Koschan, and M. A. Abidi
Imaging, Robotics, and Intelligent Systems Laboratory
The University of Tennessee
Knoxville, TN 37996
yiyong@iristown.engr.utk.edu

Abstract

This paper describes 3D mapping of indoor and outdoor environment using a mobile range scanner. In the raw range data preprocessing stage, we propose to use area decreasing flow for surface mesh smoothing instead of the mean curvature flow. Although the proposed area decreasing flow approach is mathematically equivalent to the mean curvature flow, it can avoid the difficulty in curvature estimation and provide an optimal flowing step size. Geometric details are preserved by adaptive smoothing on crease edges. In the multi-view 3D reconstruction stage, we combine the space carving with Hilton's implicit surface-based method to generate watertight 3D models from limited number of scans. Volumetric deformation by mean curvature flow using the level set method is applied in the post-processing stage to remove outliers. We present results of 3D reconstruction of real indoor and outdoor environment from multi-view noisy range data.

1. Introduction

As one of the active research areas in computer vision, 3D reconstruction has important applications in virtual reality, reverse engineering and robot vision. Although more expensive than stereo systems, laser range scanners have been widely used for 3D reconstruction tasks due to the relatively high measurement accuracy and elimination of the correspondence problem. Mounted on a remotely controlled mobile platform, the range scanner can be sent into an environment dangerous to human beings, either for the purpose of robot navigation or 3D reconstruction of the environment.

Surface reconstruction from range images involves raw range data processing, registration of surfaces into a global coordinate system, multi-view data integration, and post-processing of the reconstructed 3D model such as removing outliers and geometric simplification. In this paper, we propose new methods for raw surface mesh smoothing and multi-view data integration. Traditional methods for registration and post-processing are adopted.

The acquired range signals are usually corrupted by noise. In the preprocessing stage, surface smoothing is capable of suppressing noise and feeding improved data to successive processes. For example, our 3D integration process benefits from accurate normal estimation that is a result of effective triangle mesh smoothing. In previous works, the surface smoothing problem has been tackled in the literature using different approaches, including regularization, surface fairing, and surface evolution using the level set method. Regularization performs smoothing operations by minimizing an energy function that includes data compatibility and smoothing terms. Different definitions of the smoothing term have been proposed for surfaces of a height map [2, 14, 18]. Laplacian smoothing on a triangle mesh was applied in [15, 17]. Ohtake *et al.* showed that Laplacian smoothing tends to develop unnatural deformations and instead applied the mean curvature flow [10].

Curvature is only defined on an infinitesimal area. Robust estimation of curvature values on a triangle mesh is difficult. The step size of mean curvature flow is data dependent and usually decided by experiment. In this paper, we propose to use area decreasing flow which is mathematically equivalent to mean curvature flow. The advantage of the proposed flow is there is no curvature estimation needed and an optimal flowing step size can be solved uniquely.

Among the existing multi-view range data integration approaches, implicit surface-based methods [3, 6] are more robust to noise and registration error. Implicit surface-based methods integrate multiple surfaces by fusing implicit fields in a volume. The polygonisation of implicit surfaces guarantees the quality of the extracted triangle mesh and is more robust than mesh merging methods [13, 16]. Implicit surface-based methods utilize triangle meshes from each single view instead of only using points. The extra information of surface normal makes integration more robust than methods that reconstruct surface from unorganized points [1, 7]. Although both Curless [3] and Hilton [6] used signed distance to surface to generate implicit fields, Hilton computes the real distance from voxel to surface. However, Hilton does not use space carving which is helpful to remove outliers and generate watertight models. In this paper, we combine Hilton's approach with space carving. As a result, we are able to obtain watertight models of indoor environment by using a few range scans in spite of incomplete data from self occlusions.

2. Surface smoothing by area decreasing flow

Surface mesh smoothing is conducted by adjusting positions of vertices in a neighborhood of the original measurements. The variation of a parameterized surface $\mathbf{X}$ along normal $\mathbf{n}$ is given as $\mathbf{X}^t(u,v) = \mathbf{X}(u,v) + t\,l(u,v)\mathbf{n}(u,v)$, where $\mathbf{X} : U \subset \mathbf{R}^2 \rightarrow \mathbf{R}^3$, $(u,v) \in U$, $t \in (-\varepsilon, \varepsilon)$, and l is a differentiable function.

For an umbrella neighborhood with I triangles on a triangle mesh, the position of the center vertex $\mathbf{v}$ is adjusted along $\mathbf{n}$, as shown in Fig. 1(a). The original center vertex position is denoted as $\mathbf{v}^{(0)}$. In the k-th adjustment, the center vertex moves from $\mathbf{v}^{(k)}$ to $\mathbf{v}^{(k+1)}$ by the length l in the direction of $\mathbf{n}^{(k)}$, such as

$$\mathbf{v}^{(k+1)} = \mathbf{v}^{(k)} + l\,\mathbf{n}^{(k)}. \qquad (1)$$

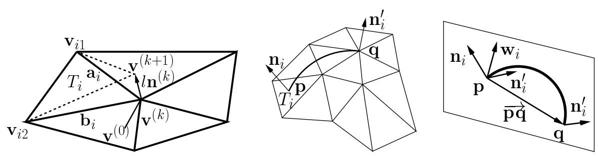

Figure 1. (a) Move $\mathbf{v}^{(k)}$ to $\mathbf{v}^{(k+1)}$ to minimize the umbrella area. (b) $\mathbf{n}'_i$ is the voted normal by $\mathbf{n}_i$. (c) Normal transportation.

Traditional surface mesh smoothing based on mean curvature flow [4, 10] sets $l = \alpha H$, where H is the mean curvature, and $\alpha > 0$ and is determined by experiments. Surface mesh smoothing is treated as a regularization problem in this paper. It involves minimizing an energy function: $f(\mathbf{X}) = h(\mathbf{X}) + \lambda g(\mathbf{X})$, where minimization of $g(\mathbf{X})$ involves the compatibility of the solution to the original observation, and minimization of $h(\mathbf{X})$ incorporates prior knowledge. λ is called the regularization parameter. The smoothness is assumed to be the prior knowledge of the surface.

We choose $h(\mathbf{X})$ to be the surface area A_s of $\mathbf{X}$. This is closely related to the mean curvature flow because the derivative of area $A_s(t)$ of $\mathbf{X}^t$ at $t = 0$ can be obtained as $A'_s(0) = -\int 2\,l\,H\sqrt{EG - F^2}du\,dv$, and the area is always decreasing if the normal variation is set as $l = \alpha H$, where E, F and G are the coefficients of the first fundamental form [5].

The curvature on a triangle mesh is difficult to compute because it is defined on an infinitesimal area. However, direct surface area minimization can avoid curvature estimation and an optimal solution of l can be uniquely obtained.

The data compatibility term $g(\mathbf{X})$ is chosen to be the square of the distance that a vertex moves. Thus, the energy function is defined as

$$f(l) = \sum_{i=1}^{I} 4[S_i^{(k+1)}]^2 + \lambda\,\|\mathbf{\Delta v}^{(k+1)}\|^2, \qquad (2)$$

where $S_i^{(k+1)}$ is the area of the triangle T_i and computed as $S_i^{(k+1)} = \frac{1}{2}\|(\mathbf{v}_{i1} - \mathbf{v}^{(k+1)}) \wedge (\mathbf{v}_{i2} - \mathbf{v}^{(k+1)})\|$, where $\wedge$ denotes cross product, and $\mathbf{\Delta v}^{(k+1)}$ is defined as $\mathbf{\Delta v}^{(k+1)} = \mathbf{v}^{(k+1)} - \mathbf{v}^0$. The optimum value of step size l, which minimizes f, can be obtained by solving $\frac{\partial f}{\partial l} = 0$ as

$$l = \frac{A - \lambda\,\mathbf{\Delta v}^{(k)} \cdot \mathbf{n}^{(k)}}{B + \lambda}, \qquad (3)$$

where $A = \sum_{i=1}^{I}\{(\mathbf{b}_i \cdot \mathbf{n}^{(k)})\mathbf{a}_i - (\mathbf{a}_i \cdot \mathbf{n}^{(k)})\mathbf{b}_i\} \cdot (\mathbf{a}_i - \mathbf{b}_i)$, $B = \sum_{i=1}^{I}\|\mathbf{a}_i - \mathbf{b}_i\|^2 - \{(\mathbf{a}_i - \mathbf{b}_i) \cdot \mathbf{n}^{(k)}\}^2$, $\mathbf{a}_i = \mathbf{v}_{i1} - \mathbf{v}^{(k)}$, and $\mathbf{b}_i = \mathbf{v}_{i2} - \mathbf{v}^{(k)}$.

To preserve crease edges on the triangle mesh, we make the smoothing adaptive by modifying (1) into $\mathbf{v}^{(k+1)} = \mathbf{v}^{(k)} + e^{-5s}\,l\,\mathbf{n}^{(k)}$, where s represents the edge strength at a vertex. We propose a method to compute s for each vertex on a triangle mesh based on Medioni's tensor voting method [9].

For a certain vertex $\mathbf{q}$, the votes are cast by the neighboring triangles, as shown in Fig. 1(b). The voted tensor cast by the triangle T_i at $\mathbf{q}$ is $\mu_i \mathbf{n}'_i {\mathbf{n}'_i}^T$, where $\mathbf{n}'_i$ is the voted normal by T_i's normal $\mathbf{n}_i$ and μ_i is the weight of the vote. The new tensor collected at $\mathbf{q}$ is $\mathbf{T} = \sum_{i=1}^{M} \mu_i \mathbf{n}'_i {\mathbf{n}'_i}^T$, where M is the number of triangles inside a geodesic window of $\mathbf{q}$ and $M > I$, and the weight μ_i exponentially decreases according to the geodesic distance between $\mathbf{p}$ and $\mathbf{q}$. $\mathbf{n}'_i$ is obtained by transporting $\mathbf{n}_i$ through a sector of arc connecting $\mathbf{p}$ and $\mathbf{q}$ where $\mathbf{p}$ represents the centroid of T_i. Fig. 1(c) illustrates the voting process. The arc is on the plane defined by vectors $\mathbf{n}_i$ and $\overrightarrow{\mathbf{pq}}$. The normals at two terminals of the arc are $\mathbf{n}_i$ and $\mathbf{n}'_i$. $\mathbf{n}'_i$ is computed as $\mathbf{n}'_i = 2(\mathbf{n}_i \cdot \mathbf{w}_i)\mathbf{w}_i - \mathbf{n}_i$, where $\mathbf{w}_i = \frac{(\overrightarrow{\mathbf{pq}} \wedge \mathbf{n}_i) \wedge \overrightarrow{\mathbf{pq}}}{\|(\overrightarrow{\mathbf{pq}} \wedge \mathbf{n}_i) \wedge \overrightarrow{\mathbf{pq}}\|}$. The normal transportation is less accurate when the geodesic distance between $\mathbf{p}$ and $\mathbf{q}$ is too large. μ_i makes the voting rely more on the vertices nearby.

We define the crease edge strength as

$$s = \begin{cases} 1, & \text{if } |\overline{\mathbf{n}} \cdot \mathbf{e}_1| < \delta \\ (\nu_2 - \nu_3)/\nu_1, & \text{otherwise} \end{cases}, \qquad (4)$$

where $\nu_1 \geq \nu_2 \geq \nu_3$ are eigenvalues of $\mathbf{T}$, $\mathbf{e}_1$ is the eigenvector corresponding to ν_1, and $\overline{\mathbf{n}} = \sum_{i=1}^{M} \mu_i \mathbf{n}'_i$. In the experiments, the smoothing results are usually obtained less than five iterations. However, more sophisticated convergence criteria can be used instead.

3. Multi-view 3D integration

In most cases, it is impossible to take complete range scans of indoor or outdoor environment due to self occlusion. Generally, there are more self occlusions in an outdoor environment. For example, when the range scanner is positioned on the ground, the top of buildings can not be scanned. Space carving method fills the space whenever a step discontinuity is encountered so that a watertight 3D model can be generated. Space carving is not proper for outdoor 3D reconstruction where a lot of deep step discontinuities exist. Leaving the holes where no data are available generates more reasonable 3D models. However, space carving is very useful in indoor reconstruction where most surfaces can be scanned.

We reconstruct outdoor scene using Hilton's implicit surface-based method [6], which is briefly described as follows:

1. A volumetric grid is initialized to contain the region of interest. A surface mesh is generated from each range image and a k-D tree data structure is built for all the vertices of the mesh.

2. The voxels near the surface mesh are located and their indices are put into a queue Q.

3. For each voxel $\mathbf{x}$ in the queue, its nearest point $\mathbf{p}$ on the surface mesh is obtained from the query of the k-D tree. The signed distance between the voxel and the surface mesh is computed as the dot product of $\overrightarrow{\mathbf{xp}}$ with $\mathbf{n}$, which is the normal vector at $\mathbf{p}$. When a new surface is to be integrated, the signed distance field is updated by the weighted average according to the confidence of the measurement.

4. The final surface mesh is extracted using the marching cube algorithm [8].

The 3D models reconstructed by this method often contain holes due to incomplete data. For indoor environment reconstruction, we combined an additional space carving with Hilton's method to generate watertight model. Knowing the calibration of the range scanner, for each voxel in the space, we can find its corresponding pixel in the range image based on the back projection. Assume the distance between a voxel and the camera is R_v and the range value stored in the projected pixel is R_i. The voxel is marked as empty if the voxel is not in Q and $R_v < R_i$. The holes are filled by carving out the empty space. The multi-view integration and surface extraction still only involve the voxels in Q. Curless and Levoy [3] used $R_v - R_i$ to compute the signed distance field. In spite of efficiency, it is not the real voxel-surface distance and implicit fields obtained from different viewpoints are not continuous because they are not measured along the surface normal direction.

After reconstruction, the surface is post-processed to remove outliers by mean curvature flow using the level set method [12] in a volumetric grid.

4. Experimental results

The range data shown in this paper were captured by the RIEGL laser scanner LMS-Z210 [11]. Fig. 2(a)-2(d) show the two-view range images in front of a building, noisy surfaces obtained from first range image, adaptive smoothing result in which geometric details are preserved, and the 3D reconstruction with 159,677 triangles.

Fig. 3(a)-3(d) show the RIEGL scanner on a mobile platform, a corner of a room, the four-view 3D reconstruction result with 341,639 triangles, and the simplified model with 5,000 triangles.

5. Conclusions

We presented a system for 3D reconstruction of indoor and outdoor environment from multi-view range data. The area decreasing flow is proposed for surface mesh smoothing. Direct area minimization avoids mean curvature estimation and an optimal flowing step size can be solved uniquely. Crease edge strength of each vertex is computed by eigen analysis of normal vectors on the triangle mesh. Geometric details are preserved by regularized adaptive smoothing on the crease edges. For outdoor environment reconstruction, the smoothed surface meshes from multiple views are integrated using Hilton's method, which fuses the implicit field in the volumetric grid. For indoor environment reconstruction, we showed that additional space carving is effective to generate watertight models in spite of incomplete surface scans. Results of 3D reconstruction of real indoor and outdoor environment from multi-view noisy range data are presented.

Acknowledgement

This work was supported by the University Research Program in Robotics under grant DOE-DE-FG02-86NE37968, by the DOD/TACOM/NAC/ARC Program, R01-1344-18, and by FAA/NSSA Program, R01-1344-48/49.

References

[1] F. Bernardini, J. Mittleman, H. Rushmeier, C. Silva, and G. Taubin. "The ball-pivoting algorithm for surface recon-

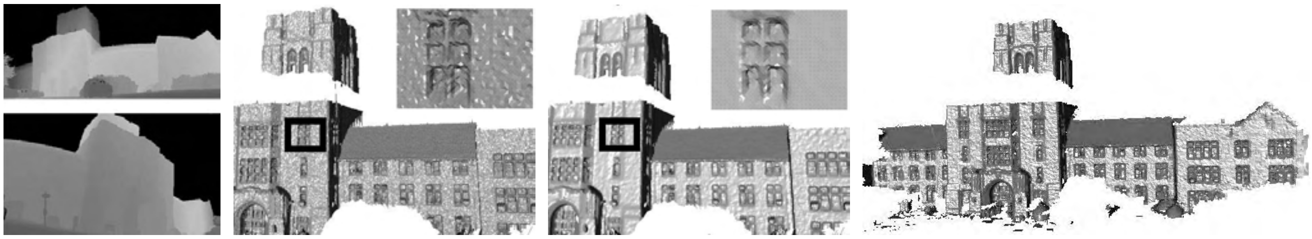

(a) (b) (c) (d)

Figure 2. (a) Range images from two views. (b)(c) Original raw surface and adaptive triangle mesh smoothing result using area decreasing flow, with magnified details from window. (d) 2-view 3D reconstruction without space carving, 159,677 triangles.

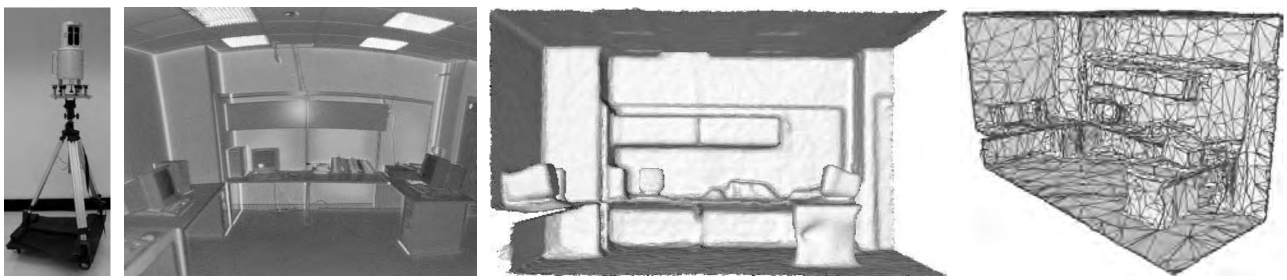

(a) (b) (c) (d)

Figure 3. (a) RIEGL Scanner on a mobile platform. (b) A corner of room to be reconstructed. (c) Four-view watertight 3D reconstruction of (b) with space carving, 341,639 triangles. (d) Simplified model of (c) with 5,000 triangles.

struction". *IEEE Trans. Visualization and Computer Graphics*, 5:349–359, 1999.

[2] A. Blake and A. Zisserman. *Visual Reconstruction*. Cambridge, Mass.: MIT Press, 1987.

[3] B. Curless and M. Levoy. "A volumetric method for building complex models from range images". In *Proc. SIGGRAPH*, pages 303–312, 1996.

[4] M. Desbrun, M. Meyer, P. Schroder, and A. H. Barr. "Implicit fairing of irregular meshes using diffusion and curvature flow". In *Proc. SIGGRAPH*, pages 317–324, 1999.

[5] M. DoCarmo. *Differential Geometry of Curves and Surfaces*. Prentice Hall, 1976.

[6] A. Hilton, A. Stoddart, J. Illingworth, and T. Windeatt. "Implicit surface-based geometric fusion". *Computer Vision and Image Understanding*, 69:273–291, 1998.

[7] H. Hoppe, T. Derose, and T. Duchamp. "Surface reconstruction from unorganized points". In *Proc. SIGGRAPH*, volume 26, pages 71–78, 1992.

[8] W. E. Lorensen and H. E. Cline. "Marching cubes: A high resolution 3d surface construction algorithm". In *Proc. SIGGRAPH*, pages 163–169, 1987.

[9] G. Medioni, M. S. Lee, and C. K. Tang. *A Computational Framework for Segmentation and Grouping*. Elsevier Science B.V., 2000.

[10] Y. Ohtake, A. Belyaev, and I. Bogaevski. "Polyhedral surface smoothing with simultaneous mesh regularization". In *Proc. Geometric Modeling and Processing*, pages 229–237, 2000.

[11] RIEGL Laser Measurement Systems. *Laser Mirror Scanner LMS-Z210, Technical Documentation and User's Instructions*, 2000.

[12] J. A. Sethian. *Level Set Methods and Fast Marching Methods: Evolving Interfaces in Computational Geometry, Fluid Mechanics, Computer Vision and Material Sciences*. Cambridge University Press, second edition, 1998.

[13] M. Soucy and D. Laurendeau. "A general surface approach to the integration of a set of range views". *IEEE Trans. Pattern Anal. Machine Intell.*, 17:344–358, Apr. 1995.

[14] R. L. Stevenson and E. J. Delp. "Viewpoint invariant recovery of visual surface from sparse data". *IEEE Trans. Pattern Anal. Machine Intell.*, 14(9):257–270, Sept. 1992.

[15] G. Taubin. "A signal processing approach to fair surface design". In *Proc. SIGGRAPH*, pages 351–358, 1995.

[16] G. Turk and M. Levoy. "Zippered polygon meshes form range images". In *Proc. SIGGRAPH*, pages 311–318, 1994.

[17] J. Vollmer, R. Mencl, and H. Muller. "Improved Laplacian smoothing of noisy surface meshes". In *Proc. Eurographics*, pages 131–138, 1999.

[18] J. H. Yi and D. M. Chelberg. "Discontinuity-preserving and viewpoint invariant reconstruction of visible surface using a first order regularization". *IEEE Trans. Pattern Anal. Machine Intell.*, 17(6):624–629, June 1995.

1051-4651/02 $17.00 (c) 2002 IEEE